IOP Publishing Physica Scripta
Phys. Scr. **86** (2012) 045009 (10pp) doi:10.1088/0031-8949/86/04/045009

Curl-free vector potential observation on the macro-scale for charged particles in a magnetic field compared with that on the micro-scale: the Aharonov–Bohm effect

Ram K Varma

Physical Research Laboratory, Navrangpura, Ahmedabad 380 009, India

E-mail: ramkvarma@gmail.com

Received 26 July 2012
Accepted for publication 12 September 2012
Published 8 October 2012
Online at stacks.iop.org/PhysScr/86/045009

Abstract
The recently reported curl-free vector potential observation (Varma *et al* 2012 *Eur. Phys. J.* D **66** 38) in relation to a system of charged particles in a magnetic field points to the existence of a new state of the electron—a quantum modulated state—which arises through a scattering-induced transition across Landau levels. This quantum modulated state has been shown to account for some very unusual effects on the macro-scale, which are distinct from the ones which can be understood in terms of a 'classical electron' and also from the ones which can be understood in terms of a 'quantum electron' on the micro-scale characterized by the Planck quantum. This quantum modulated state has been shown to account for the observation of a static curl-free vector potential on the macro-scale alluded to above, as well as other matter wave manifestations on the macro-scale. The macro-scale curl-free vector potential observation differs fundamentally from the corresponding micro-scale effect—the well-known Aharonov–Bohm effect. These two effects—on the macro-scale and the macro-scale—are compared and contrasted to each other here in their manner of detection of the static curl-free vector potential. Such a comparative study helps gain a deeper understanding of the nature of the quantum modulated state and the macro-scale matter wave it represents.

PACS numbers: 03.75.−b, 03.65.Ta, 41.75.Fr

1. Introduction

The Aharonov–Bohm (A–B) effect is now a well-established effect pertaining to the observation of a static curl-free vector potential. This effect, proposed by Aharonov and Bohm [1], was disbelieved for a long time because of its being contrary to the then existing perception that a vector potential *per se* is not a physically observable entity unless it has an associated magnetic field, and which alone was regarded as an observable as per the entrenched Heaviside–Hertz formulation of electromagnetism. Such reservations and disbeliefs were laid to rest when Tonomura *et al* [2] conclusively demonstrated the existence of this effect by using a magnetized micro-torus which ruled out any leakage field effects that were being invoked to cast doubts on an earlier demonstration by Chambers [3], who had used a finite length magnetized whisker in his experiment.

The experiment clearly demonstrated its existence, thereby validating the nature of the effect as being due to a phase shift induced by a magnetic flux enclosed by the two interfering paths. It was thus established that it is essentially a quantum effect, and can only manifest as a shift of the fringes which is proportional to the enclosed flux. However, implicit in it was the continued belief that on the macro-scale, regarded historically as the domain of classical physics, a curl-free vector potential still does not enjoy the status of an observable. This view has recently been challenged notably by Rousseaux *et al* [4] with some support from a remark by Feynman *et al* [5]. It has been argued that an induced electric field exists even in a magnetic-field-free region, where there is a time-varying vector potential, such as, for example, in the vicinity of a magnetized torus, or an infinite magnetized cylinder. In fact, the corresponding induction equation involving the magnetic field **B** would give a null

 © 2012 The Royal Swedish Academy of Sciences

result for the induction electric field in the magnetic-field-free region, since $\partial\mathbf{B}/\partial t$ would be zero where $\mathbf{B}$ is zero. Thus even a curl-free vector potential is 'real', at least if it is time varying, because its time derivative implies an induced electric field. But, what about a static curl-free vector potential? Is it an entity devoid of any physical significance on the macro-scale, regarded as the domain of classical physics, because it can register no observable effect on a charged particle as per the Lorentz equation of classical physics?

In a recently reported experiment [6], the author and his co-workers have shown that a *static* curl-free vector potential too can affect the dynamics of a charged particle on the macro-scale. The experimental results reported here (also reported earlier [7] with a limited parameter exploration) involve parameter ranges that can only be characterized as 'classical': the dimensions of the system apparatus (length ∼50 cm, diameter ∼10 cm, the diameter of the magnetized torus producing the curl-free vector potential ∼10 cm, located outside the experimental chamber), the external magnetic field $B \sim 30$–50 G, etc. As such, an experiment such as this would, by all conventional accounts, be classified as being 'classical'; but clearly its results cannot be understood in the framework of classical physics, because the Lorentz equation as the governing equation would not permit such an effect.

However, as has been elaborated in [6], the observation of the (static) curl-free vector potential on the macro-scale, as reported there, does not belong to classical physics despite being on the macro-scale, but rather paradoxically, it has a quantum origin. In fact, the existence of this effect was predicted by a theory of the present author [8], and the subsequent observation thereof constitutes a validation of the prediction. The above-mentioned observation appears to be so enigmatic, because it goes entirely against a number of currently well-accepted tenets and perceptions. It is, therefore, pertinent to clarify the nature and origin of this effect to point out what particular perceptions need to be relaxed to accommodate these results, which are seen to posit against the canonical viewpoint. The situation is similar to the one corresponding to the A–B effect, which led ultimately to the revision of the concept of the observability of the curl-free vector potential, although only quantum mechanically. The present situation will be seen to be even more critical, because the observations—of the vector potential—here go beyond the micro-scale of quantum physics well into the macro-scale, regarded conventionally as the domain of classical physics.

Thus with reference to the curl-free vector potential observation, one can now distinguish three different modes in which the electron seems to manifest itself: two of them have so far been:

(i) A 'classical electron' whose dynamics is governed by the Lorentz equation, regarded as the descriptor of electrodynamic phenomena on the macro-scale. In particular, a static curl-free vector potential cannot affect its motion, because the Lorentz equation involves only a magnetic field, which vanishes, by definition, for a curl-free vector potential.

(ii) The 'quantum electron' which displays, in addition to its particle attributes, a matter wave property which comes into play on the micro-scale. This has well-known consequences on the micro-scale, such as the matter wave interference effects. In fact, the whole gamut of quantum phenomena are a consequence of this wave property. In the context of the present discussion, however, this micro-scale (wave) property of the electron has enabled a curl-free vector potential to be observable on the micro-scale of $\hbar$ (the A–B effect), which is denied by the 'classical' electron.

(iii) As mentioned above, some recently reported results on the charged particle dynamics have led to unravelling of a third mode of electron behaviour, which belongs ostensibly to neither of the above two categories. It manifests on the macro-scale, but is certainly not classical. It is not quantum in the usual sense, in that nowhere does it involve an $\hbar$ as a quantum signature. But it does exhibit matter wave effects, but on the macro-scale, as against the micro-scale matter wave. The most dramatic manifestation of this is in the observation of a curl-free vector potential as reported in [6].

The observation of a curl-free vector potential thus serves as a critical reference phenomena with respect to which these three modes of the electron behaviour can be analysed and understood. Since the first two modes are already well understood with respect to each other, we shall only consider a comparative analysis involving the latter two. We shall identify the elements of commonality between the two, and more importantly the differences which make them so radically apart. In the process, we shall be led to examine the different nature of these effects. We shall begin by recounting the various observational characteristics of the two, even at the cost of some redundancy.

2. The A–B effect

The A–B effect is so well known that it need not be described here in detail. The basic premise of the effect is that the wave function of a particle (the electron) acquires a phase of amount $\phi_1(x) = e\int_1^x \mathbf{A}\cdot\mathbf{d}\ell/c\hbar$ as the particle traverses through the region from the slit '1' to the point of observation $\mathbf{x}$. Traversing from the other slit '2' to the same point of observation $\mathbf{x}$ along another path, it acquires the phase $\phi_2(x)$, similarly defined. If these paths happen to lie in a multiply connected domain defined by a sharply enclosed region of non-zero magnetic flux, and are not reducible to each other, then the interference term arising from the interference of these two paths acquires an additional phase determined by the flux Φ thus enclosed by the two interfering paths topologically, and which equals $e\Phi/c\hbar$. This consequently manifests as a shift of the entire fringe pattern—referred to as the A–B shift.

The following are considered the defining characteristics of the A–B effect.

(i) It is obviously a quantum effect, as evidenced from the presence of $\hbar$ in the phase shift, and is essentially a consequence of the wave property of the electron.

(ii) It is regarded as of topological origin because of the multiply connected nature of the space induced by the presence of a region enclosing the magnetic flux. Such a multiply connected domain is essential for the existence of the effect. As such, it requires a minimum of two

spatial dimensions. Also, the magnetic flux enclosing region needs to intervene between the slits and the observation screen, so that the two interfering paths can go around the two sides of the topologically isolated region.

(iii) The phase shift is entirely independent of the electron energy so that the same shift, determined essentially by the flux enclosed, would occur regardless of the wavelength of the primary de Broglie wave. Also, the phase shift is proportional to the total flux enclosed.

3. The macro-scale vector potential observation

We next describe the characteristic features of the macro-scale observation of the curl-free vector potential, so that these can be compared and contrasted with those of the A–B as recounted above. Such a description would, however, have to involve a slightly greater elaboration, because of the recent discovery and consequent general unfamiliarity of this effect. Even though the manner of observation of this macro-scale effect has been well described in [6], it will be briefly described here in the present context so as to make this presentation self-contained.

If one follows the method of observation for the detection of a curl-free vector potential on the macro-scale as described in [6], it will be evident that, given the macro-scale of the entire experiment, the latter would appear to manifestly belong to the classical domain. Therefore, the canonical view will demand that the results of the experiment be understood in classical terms. However, it is obvious that an explanation in classical terms would not be feasible, because classical physics does not permit a curl-free vector potential to affect the electron dynamics. We therefore describe here the essential points of the vector potential observation on the macro-scale along with an outline of the theoretical formalism.

The system in which such an observation has been made pertains to charged particle dynamics in a magnetic field. In particular, it is the quantum structure of the system which defines the problem, specified by the bound Landau states in the perpendicular direction and plane wave states along the magnetic field. The essential point emerging out of the studies carried out is that the quantum structure of the system plays a defining role even when the magnetic field is not large, contrary to the general impression that the Landau level structure becomes significant and meaningful only at large magnetic fields.

The single feature common to both the effects—the micro-scale one and the macro-scale one—is that both arise from a matter wave property involving interference effects and phase shifts. In the case of the former it is, of course, the de Broglie wave associated with the electron which comes into the picture. As has been elaborated in [6], it is an entirely different kind of matter wave in the latter case: it is a matter wave associated with the 'quantum modulation' of the de Broglie wave—the plane wave state along the field line. The interesting manner in which such a modulation comes about has been described in detail in [9]. Basically, it arises as a consequence of transitions across a Landau level interval n, which can be induced as a result of a scattering that a particle may suffer in its journey from an electron gun to a detector plate. The quantum entanglement between the 'parallel' and perpendicular degrees of freedom then leads to a concomitant modulation of the parallel dynamics—resulting in the modulational wave. As shown in [9], such a modulational matter wave has a macro-scale wavelength with an expression $\lambda_{\rm M} = 2\pi v/\Omega$ which is clearly $\hbar$ independent and is on the macro-scale. For a magnetic field of $B \simeq 100\,{\rm G}$ and an electron energy $\mathcal{E} \sim 1\,{\rm keV}$, $\lambda_{\rm M} \simeq 5\,{\rm cm}$. The existence of such a macro-scale matter wave, associated with the modulation, has been demonstrated conclusively through the observation of matter wave interference effects with this wavelength [10, 11].

Thus the upshot is that the vector potential observation on the macro-scale is mediated by this macro-scale modulational wave, as against the A–B one, which is attributed to the de Broglie wave. This is really the chief difference between the two effects. But there are other characteristic points of differences as well, which we shall discuss.

The detection of the vector potential on the macro-scale was actually predicted by a formalism developed by the author which furnished an evolution equation for the modulation as a consequence of a Landau level transition [8]. This equation is given by

$$\frac{{\rm i}\,\mu}{n}\frac{\partial\Psi(n)}{\partial t} = \frac{1}{2m}\left(\frac{\mu}{{\rm i}\,n}\frac{\partial}{\partial x} - \frac{e}{c}\hat{A}_x\right)^2 \Psi(n) + \mu\Omega\Psi(n), \quad (1)$$

where $\Psi(n)$ denotes the wave amplitude of the modulation of the de Broglie wave along the magnetic field, $\mu = \mathcal{E}_\perp/\Omega$, the gyro-action of the injected particles, with $\mathcal{E}_\perp$ being the energy in the perpendicular component, and $\Omega = eB/mc$, the gyro-frequency in a magnetic field B. The index n here denotes the Landau level interval spanning the transition. All the equations for the different n are independent of each other, and represent different transitional states. The above equations are, interestingly, of the Schrödinger form in one dimension along the field, indicating that they represents a modulation of the one-dimensional plane wave state along the field in the x-direction. Most importantly, from the point of view of the present discussion, they carry in them the x-component of a curl-free vector potential, in the same manner as it appears in the Schrödinger equation. These equations may thus be regarded as the macro-scale Schrödinger-form wave equations for the modulation.

The presence of this vector potential component in this equation in the same manner as in the Schrödinger wave equation led to the prediction of the observation of a curl-free vector potential on the macro-scale. The macro-scale nature of the predicted effect arises from the presence of the macro-scale action μ in lieu of $\hbar$ in the above equation.

Shortly after the above-mentioned prediction, the observation of such a macro-scale detection was reported in [7]. However, some additional characteristic features of the detection were discovered later, subsequent to a theoretical investigation by the author [12] relating to the generation of the modulation, and the point of its origin. Following this analysis, the various characteristic features of the macro-scale detection were then delineated in [13]. The latest paper on the observation of the macro-scale effect [6] then reports a comprehensive validation of all the characteristic features delineated in [13].

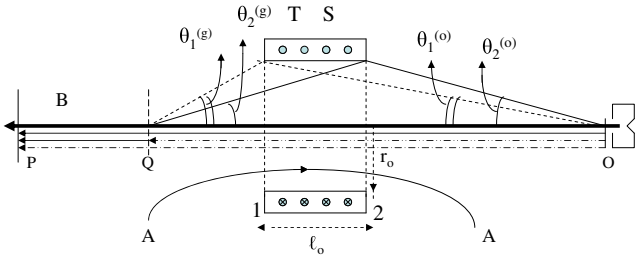

Figure 1. Schematic representation of the experimental system consisting of a vacuum chamber of length ∼50 cm and 10 cm diameter, with a high vacuum of $\sim 5 \times 10^{-7}$ Torr with an electron gun at O, the detector plate at P and a movable grid at Q. The bold solid line represents the external magnetic field. TS represents the toroidal solenoid with a rectangular cross-section (width $\ell_o = 58$ mm, thickness 19.25 mm, inner diameter $2r_o = 111.5$ mm, outer diameter 150 mm) which produces the curl-free vector potential with AA being its typical field line. The dotted lines running between O and Q and between O and P denote the unscattered de Broglie waves, while the thick full lines running between O and P and between Q and P represent sections of the trajectories with the transition amplitude wave. The angles $\theta_1^{(o)}$, $\theta_2^{(o)}$, $\theta_1^{(g)}$ and $\theta_2^{(g)}$ are as shown.

3.1. The method of detection and its various characteristic features

We shall now highlight how fundamentally different this detection is from the standard A–B one.

We note that because of the one dimensionality of equation (1) for the modulational wave, the entire process of detection occurs in one dimension. (Note the difference from the A–B case which requires a minimum of two dimensions.) The system itself is defined by the set of energy states (N, k), with N representing the Landau level quantum number and k representing the plane wave state along the field. This is achieved experimentally with an electron beam from an electron gun propagating along a magnetic field in a vacuum glass chamber, and with a pitch angle of injection δ such that the mean value of the gyro-action of the injected particles is given by $\mu = \mathcal{E} \sin^2 \delta / \Omega = N\hbar$, identifying μ with $N\hbar$, so that N represents the mean Landau level number occupation of the injected beam. The parallel plane wave state k is specified through the mean parallel energy of the particles, $\mathcal{E}_\parallel = (\hbar k)^2/2m$. The injected beam is thus specified in the mean by the quantum state (N, k).

To fix ideas about the nature of the experiment, figure 1 provides a schematic representation of the experimental system which consists of a vacuum glass chamber of 10 cm diameter and ∼50 cm length, having an axial magnetic field produced by a set of appropriate field coils, with an electron gun situated at one end, a detector plate at the other end and a movable grounded grid in between.

The curl-free vector potential required for the purpose of its detection is produced by a toroidally wound solenoid with a rectangular cross-section (58 mm × 19.25 mm) situated externally around the glass chamber. The current through the toroidal solenoid produces a flux which is completely trapped within it except for some possible small leakage field in its immediate vicinity. This flux then acts as a source of the curl-free vector potential field that exists in the space around. The component of this vector potential along the magnetic field is the one that will alone figure in the experiment. This corresponds to the vector potential component occurring in equation (1). Note that the source of the vector potential—the flux containing toroid—sits outside the glass chamber and far away (≃10 cm) from the path of the beam which travels along the axis of the cylindrical chamber.

By all conventional accounts, the macro-scale dimensions of the experimental system described above would characterize it as a 'classical system'. If one now switches on the electron gun to inject the electrons along the magnetic field with an appropriately small pitch angle, the presence of the curl-free vector potential and its variation produced by the flux in the toroid should not make any difference to the plate current, because the Lorentz equation, which is supposed to determine the outcome in these macroscopic dimensions, does not recognize a curl-free vector potential.

However, as we shall see, this system is now used to detect a curl-free vector potential on the macro-scale if one follows the procedure described in [6]. The rationale of this procedure has been described in detail in [13], which is based on the formalism [8] that had predicted this effect. Some elements of the system apparatus described above, which normally play a passive role in an experiment such as the above—a grounded grid in the path of the beam, for example—play here a crucial role in the very generation of the new physical entity, namely the 'modulational wave', as per the mechanism discussed in [9], and whose dynamics then results in the detection of curl-free vector potential on the macro-scale [6], as well as other phenomena [10, 11].

In fact, the modulational wave also gets generated by the perpendicular component of the accelerating field in the region of the electron-gun anode, through the process of scattering by the latter. As this modulational wave, or more precisely, the modulated de Broglie wave, traverses the region permeated by the curl-free vector potential, its wave amplitude as governed by the equation of evolution will acquire a phase determined by the line integral of the vector potential from its point of generation to the detector plate. But, as we shall see, the phase is now determined in units of the macroscopic action μ rather than the Planck quantum $\hbar$, since it is the former (in lieu of $\hbar$) which occurs in the governing Schrödinger-form equation for the modulation. Since typically $\mu \sim 10^8 \hbar$, the phase shifts calculated over large line integrals in the experiment get correspondingly reduced by this factor. It may be mentioned that, to be sure, μ does not have any fundamental significance like $\hbar$ and can vary in an experiment depending on the initial condition of injection.

If $\Psi^{(o)}(x_p)$ be the wave amplitude of the modulational wave reaching the plate after traversing the region from its point of generation at the anode with the position at x_o, then it will acquire a phase due to the presence of the vector potential, determined by the line integral of the latter over the path from the anode to the plate. Thus one would have from equation (1)

$$\Psi^{(o)}(x_p) \simeq A \exp\left(\frac{i e}{c\mu} \int_{x_o}^{x_p} A_x \, dx\right) \exp\left(\frac{i}{\mu} \int_{x_o}^{x_p} dx m v\right). \tag{2}$$

Next, consider the modulation generated through scattering by the wires of a grid Q, situated at x_g, somewhere between the gun and the plate. Then the phase acquired by the wave amplitude for the modulation emanating from the grid position, due to the presence of the vector potential along its path, is given by

$$\Psi^{(g)}(x_p) \simeq B \exp\left(\frac{i e}{c\mu}\int_{x_g}^{x_p} A_x \, dx\right) \exp\left(\frac{i}{\mu}\int_{x_g}^{x_p} m v \, dx\right). \tag{3}$$

As these two waves interfere at the plate, it leads to an interference term of the form

$$\Psi^*(x_p)\Psi(x_p) \simeq \cos\left[\frac{1}{\mu}\left(\int_{x_o}^{x_g}\frac{e}{c}A_x \, dx + \int_{x_o}^{x_g} m v \, dx\right)\right]. \tag{4}$$

This equation yields the following condition for the maxima of the probability density at the plate (which is proportional to the plate current) from the periodicity of the right-hand side:

$$\int_{x_o}^{x_g} dx \frac{1}{\mu}\left(\frac{eA_x}{c} + mv\right) = 2\pi j, \quad j = 1, 2, 3, \ldots. \tag{5}$$

It is essential to make a few related comments at this stage:

(i) The interference term here displays a 'phase shift' $\varphi = (e/c\mu)\int_{x_o}^{x_g} dx A_x$ which is not determined by a closed line integral, as in the A–B case, but by a finite length line integral over an open path difference (x_g, x_o). This is the path difference between the two open paths (x_p, x_o) and (x_p, x_g) which are those traversed by the modulational waves from their points of generation at x_o and x_g. A path difference thus arises in one dimension essentially because the paths traversed by the modulational waves are reckoned from their point of generation. It is important to fully appreciate this distinction. If it were not for this quantum modulated state of the electron, the generation of the phase shift in one dimension would appear to be quite baffling, when looked at from the conventional viewpoint prejudiced by the A–B effect. By contrast, the A–B effect involves the 'bare' electron, and multiply connectedness of the domain becomes essential for the generation of the phase shift.

(ii) Because of the above difference it does not require the flux-carrying region to be in the path of the electron beam. In fact, the flux-containing toroid is placed outside the experimental system. What one needs is merely the presence of a curl-free vector potential field which can be sensed by the modulational wave carried by the particles as they go through the region.

(iii) A consequence of the above facts is that, while in the A–B case, the total flux Φ in the flux-containing region contributes to the phase shift, because of the complete topological enclosure; in the present case of the macro-scale effect, the phase shift is determined by the line integral of the vector potential over a finite open path, being the path difference (x_g, x_o), which would yield only a fraction G of the total flux Φ contributing to the phase shift. The phase shift would then be dependent on the above path difference, and would vary with it with the variation of the position x_g of the grid. The factor G is a geometrical factor which is determined by the length of the above path difference and its location with respect to the toroid. Its expression is given in [6, 13].

(iv) Another major difference between the two effects is that while the phase shift in the case of the macro-effect is expressed in units of $\mu = \mathcal{E}_\perp/\Omega$ and therefore depends on the electron velocity; the A–B phase shift is, on the other hand, expressed in units of the Planck constant $\hbar$ and is thus independent of the electron velocity.

The vector potential-induced phase shift thus calculated would then determine the 'fringe shift' of the interference pattern in the present case, which would then signal the detection of the curl-free vector potential. The 'interference pattern' in the present case, however, is not in the spatial domain as in the A–B case, but rather in the 'wave number' or 'energy domain' because of the one dimensionality of the system. The 'interference pattern' corresponds here to the (one-dimensional) macro-scale matter wave interference effects reported in [10, 11], which have been shown to correspond to the macro-scale matter wavelength $\lambda_M = 2\pi v/\Omega$, pertaining to the modulation. Such a sequence of interference maxima/minima, reported in [11], is shown in one of our plots presented in [6]. This gives the plate current response as the electron energy is swept from a small value to a large one $\leqslant 1$ keV. The set of observed interference maxima is described by the condition

$$\frac{\Omega L_g}{v} = 2\pi\ell, \quad \ell = 1, 2, 3, \ldots, \tag{6}$$

where L_g denotes the gun–grid distance $(x_g–x_o)$.

We present in figure 2 a plot, reproduced from our paper [6, 11], depicting the macro-scale matter wave interference effects described by the above condition (6).

The required experiment is now carried out in two stages. In the first stage, an interference maximum is located in the parameter space, by fixing a certain distance L_g between the gun and the grid, turning on the electron beam with a certain energy in the range of 600–1200 eV and tuning the external axial magnetic field so as to achieve an interference maximum (say, corresponding to $\ell = 1$) in equation (6). This is like putting a detector in the A–B case at the position of a particular interference fringe to locate it.

Keeping the system tuned at this position, the current I in the toroidal solenoid is now swept from zero to a certain suitable value. This would lead to a change $\Delta\Phi$ of the flux Φ in the toroid. Since no change of energy is involved in sweeping the current I, the condition (5) for the plate current maximum reduces to

$$\frac{e}{c\mu} G\Delta\Phi = 2\pi\Delta\nu, \quad \Delta\nu = 1, 2, 3, \ldots, \tag{7}$$

where the integral $\int_{x_o}^{x_g} dx A_x$ has been evaluated in the Coulomb gauge to yield $G\Phi$, with G being a geometrical factor, and Φ the total flux in the toroid. $\Delta\Phi$ represents a change in Φ effected by a change ΔI in the current I in the toroid. The expression on the left represents the change in the phase of the wave amplitude induced by the vector potential due to a change in the current I.

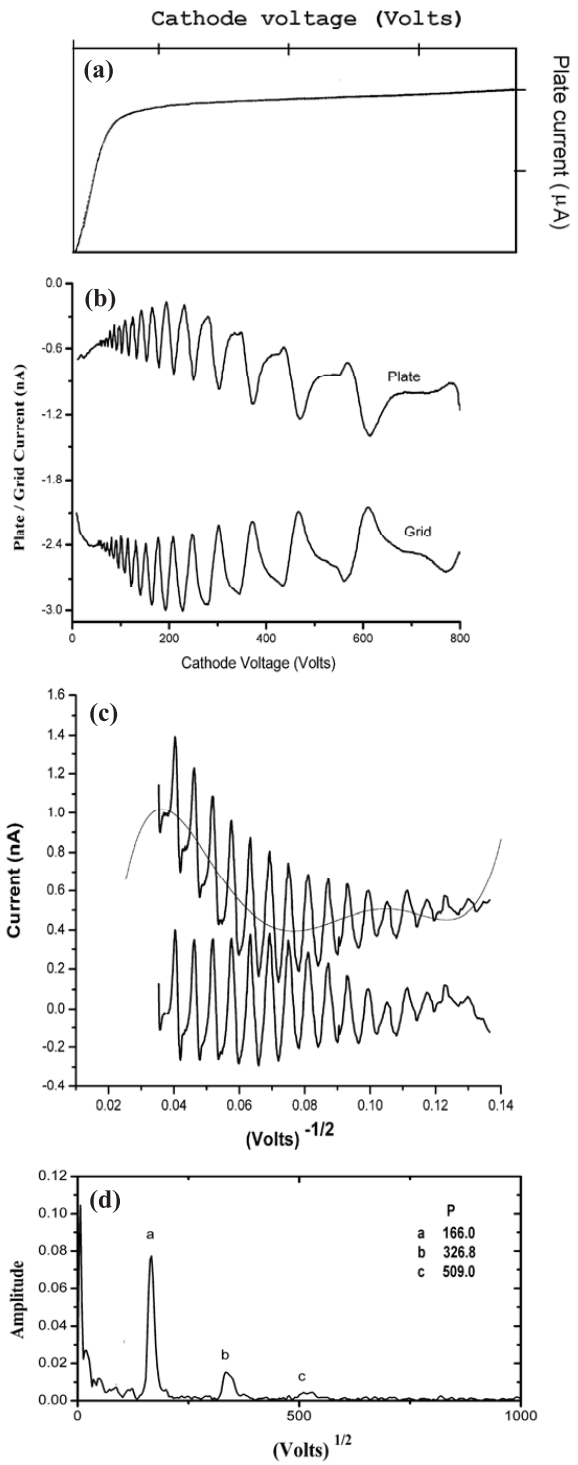

Figure 2. Plate/grid current variation as a function of electron energy. (a) Monotonic response of plate current with the monotonic sweep of electron energy $\mathcal{E}$ as expected according to Lorentz dynamics. (b) Actually observed plate and grid current responses. (c) Plate current response of panel (b) replotted as a function of $\mathcal{E}^{-1/2}$. This yields equally spaced peaks. (d) Fourier plot of curves of panel (c) showing a dominant frequency peak and two non-dominant peaks corresponding to second and third harmonics.

If one incorporates into equation (7), condition (6) for the chosen interference maximum $\ell = 1$, one obtains

$$\Delta I = \frac{mvcL_\mathrm{p}}{2e\Gamma G}\frac{B_\mathrm{p}}{B_o}\sin\delta\tan\delta\Delta\nu, \quad \Delta\nu = 1, 2, 3, \ldots, \qquad (8)$$

where the expression for $\mu = \mathcal{E}\sin^2\delta/\Omega$ has been used, and where $\Delta\Phi = \Gamma\Delta I$ has been substituted for, with Γ representing the properties of the toroid, the number of windings in it, the permeability of its core, etc. The ΔI represents the change in the current I. The change $\Delta^{(1)}I$ corresponding to a change of order $\Delta\nu = 1$ then defines the inter-peak separation of the various maxima in the plate current when the current I is varied. For a given change in current ΔI, the vector potential-induced phase shift can be identified from equation (8) as $\varphi = \Delta I(2e\Gamma G/mvcL_\mathrm{p})(B_\mathrm{o}/B_\mathrm{p})(\sin\delta\tan\delta)^{-1}$.

Relation (8) now describes the various characteristic features of the vector potential detection which can be checked against the observations. There are two important parameters which $\Delta^{(1)}I$ involves:

(a) $\Delta^{(1)}I$ varies directly with the velocity v of the electron. Thus $\Delta^{(1)}I \sim \mathcal{E}^{1/2}$. Accordingly, the phase shift φ defined above varies inversely with the velocity $v \sim \mathcal{E}^{1/2}$. This may be contrasted with the A–B case, where the phase shift is independent of the electron energy.

(b) $\Delta^{(1)}I$ varies inversely with the geometrical factor G. There is no counterpart of this in the A–B effect. This dependence is actually uniquely characteristic of this macro-scale effect, as it reflects the dependence of the phase shift on the length of the path difference $(x_\mathrm{g}, x_\mathrm{o})$ over which the line integral of the vector potential is evaluated. This leads to the fraction G of the total flux Φ determining the phase shift. The factor G is determined by the path length $(x_\mathrm{g}, x_\mathrm{o})$ which, in turn, is specified by the positions of the gun–anode at x_o and the grid at x_g both of which are taken to act as the generators of the 'modulational waves' as outlined above. A validation of the dependence of the observed effect on the factor G would then constitute a validation of the mechanism of generation of the modulational wave.

When the experiment is carried out as stipulated above—that is, vary the current in the toroidal solenoid with the system in the tuned state, the plate current has been found to give an undulatory response with the current sweep (as against a *flat* response as per the expectations of the Lorentz equation), indicating thereby that the electrons do get affected by the change in the vector potential field through which they are propagating. This undulatory response thus signals the detection of the curl-free vector potential.

To check the quantitative dependence of the effect on the electron energy, as identified in (i) above, the experiment was carried out for various energies: $\mathcal{E} = 600$, 800, 1000, 1100 and 1200 eV, while the gun–grid distance is fixed at a certain value. The plate current response obtained in the various cases is depicted in the left-hand panel of figure 3.

The $\mathcal{E}^{1/2}$ dependence of the inter-peak separation is clearly discernible, as the latter is seen to increase with the energy. The right-hand panel of figure 3 gives the Fourier plots of the respective curves in the left-hand panel. The dominant Fourier peak (the only significant one) is seen to shift to lower 'frequency' with an increase of energy. This reflects an inverse dependence of the 'frequency' peak with the inter-peak interval and therefore with $\mathcal{E}^{1/2}$. As such, the phase shift φ as defined above is seen to decrease with the

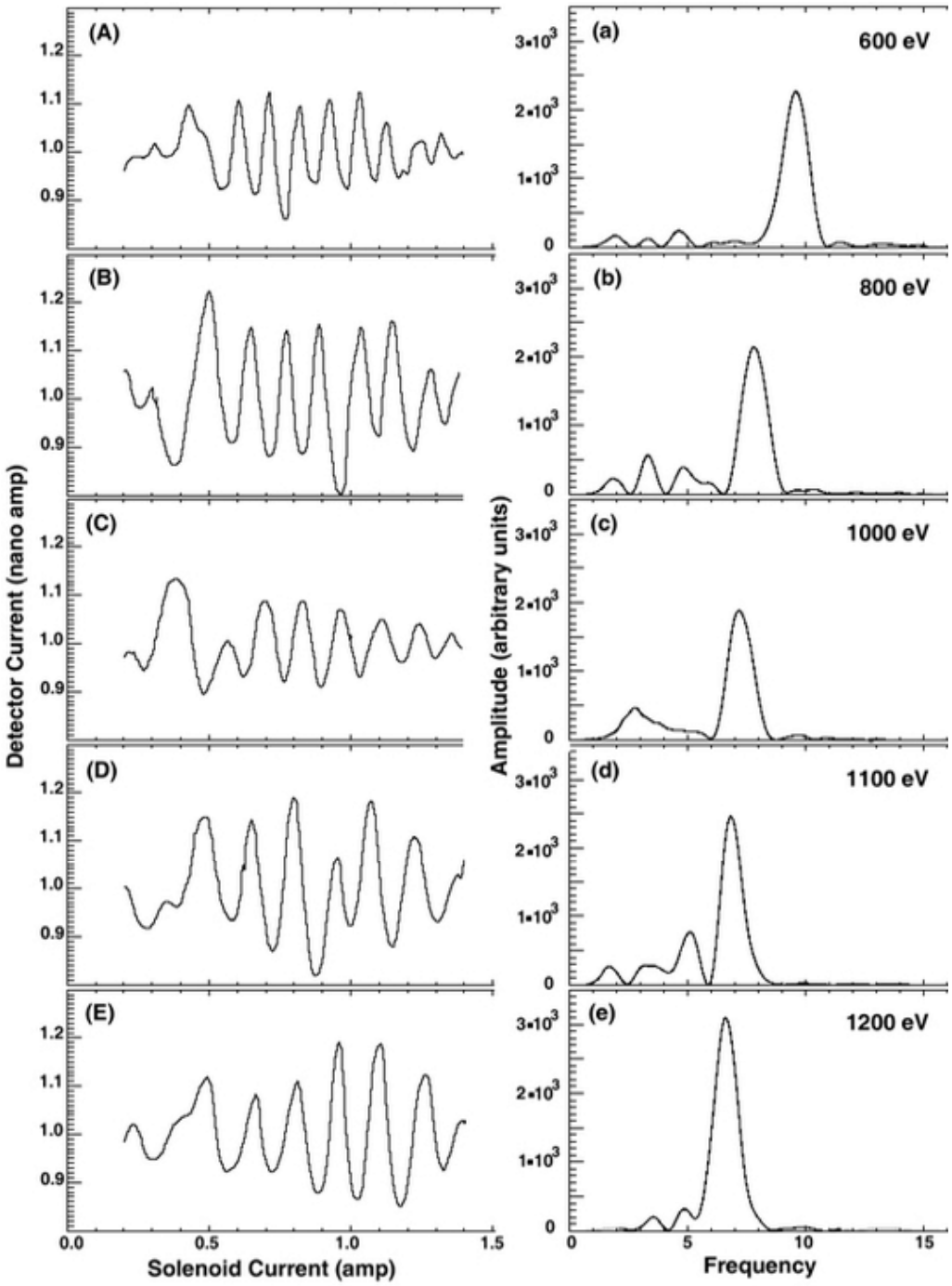

Figure 3. Detector plate current versus the current in the toroidal solenoid. The plots (A)–(E) of the left panel denote the detector current in nA plotted against the solenoidal current in amperes (A) for respectively electron energies $\mathcal{E}$(eV) = 600, 800, 1000, 1100 and 1200. These have been corrected for the saturating core, which leads to dilation in the inter-peak separation in the original plots with increasing the solenoidal current. The plots (a)–(e) denote the Fourier plots corresponding to plots (A)–(E) of the left panel.

energy as $\mathcal{E}^{-1/2}$. When the inter-peak separation $\Delta^{(1)}I$ is plotted against $\mathcal{E}^{1/2}$, for the various energies studied, the plot is shown in figure 4(A), which clearly shows the expected linear dependence, with high degree of correlation $R^2 = 0.98$.

Likewise, the G dependence of the inter-peak interval is studied by varying the position of the grid with respect to the gun (the plate position remaining fixed throughout), so that the position of one of the generating sources of the modulational wave—the grid—is varied. The electron energy is kept the same throughout at $\mathcal{E} = 830$ eV. As expected, by virtue of relation (8), the inter-peak separation $\Delta^{(1)}I$ is found to increase with a decrease of the distance (x_g, x_o). However, to compare with the precise expected dependence on G, such a dependence is calculated in [13] using the expression for G in terms of the angles as shown in figure 1. Figure 4(B) presents three curves giving the variation of $\Delta^{(1)}I$, normalized to its value for $D = 11$ cm (D being the plate–grid distance), as a function of D for three different values of the effective radius of the toroid $r_o = 5.6$, 5.8 and 6.0 cm. The curve shows a rather dramatic increase in the value of

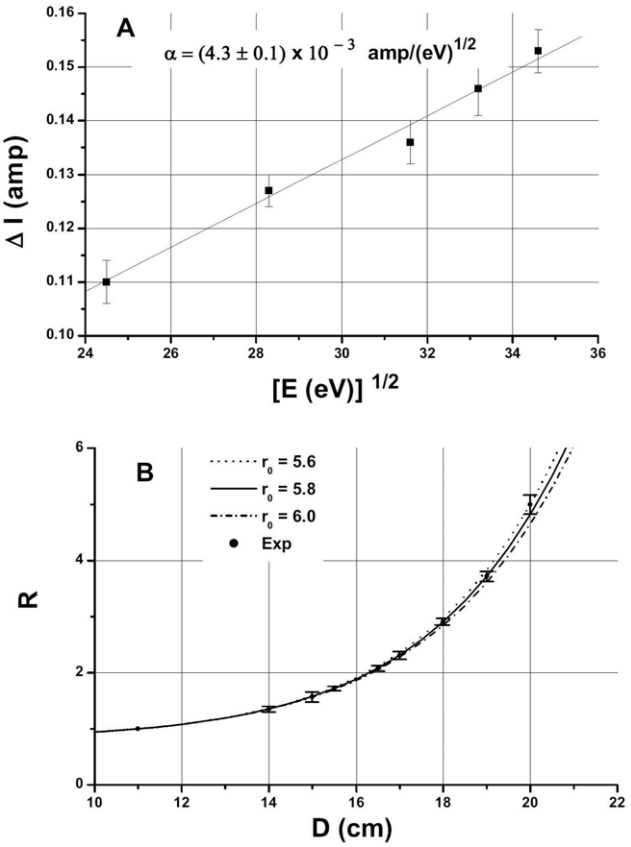

Figure 4. (A) Inter-peak solenoidal current interval ΔI against versus different electron energies. The inter peak separations ΔI depicted here, expected to be equally spaced with respect to the toroidal current. The error bars in the plots are obtained using several different runs for a given electron energy with external magnetic field values differing by 0.1 G on either side of the best value. The figure gives the plot of ΔI against the square root of electron energy $\mathcal{E}^{1/2}$, confirming the theoretically expected linear dependence. (B) The ratio $R = \Delta I_D/\Delta I_{11}$ for the various distances D (cm) for the same energy $\mathcal{E} = 830$ eV. The various curves (continuous, dotted, dashed-dotted) are the theoretical ones, with the 'dots' being experimental points.

the normalized inter-peak interval with an increase in the value of D.

We have not shown here the curves depicting the plate current response as a function of the current in the solenoid for different plate–grid distances D for a given energy $\mathcal{E} = 830$ eV. These can be looked up in [6]. But the experimentally determined inter-peak intervals normalized to its value for $D = 11$ cm are indicated as points—with appropriate error bars—in the plot of figure 4(B). There is seen to be excellent agreement between these points and the calculated curve corresponding to the effective radius $r_o = 5.8$ cm. The dependence of the inter-peak interval $\Delta^{(1)} I$ on the geometrical factor G thus stands rather closely validated.

4. Comparison between the micro-scale (A–B) and the macro-scale vector potential detection

Having described the observed characteristics of the macro-scale-vector potential detection, we now summarize them in relation to those of the known A–B effect. We have described above the experimental demonstration of the characteristics already spelt out in points (i)–(iv) above following equation (4). The following summary highlights some of these points put somewhat differently:

1. The first thing to note about these effects is that while the micro-scale A–B effect is observed in a magnetic field free space, which has only a topologically isolated flux-enclosing region, between the slits and the observation screen. The macro-scale effect as described here, on the other hand, is actually defined only through the context of a system of charged particles in a magnetic field. The curl-free vector potential field is superposed over the latter and is detected in the manner described herein, where the magnetic field is held strictly constant when the vector potential field is varied. This ensures that the effects observed are due purely to the variation of the latter.
2. The A–B effect is observed through the wave property of the electron à la de Broglie, and uses, in the simplest arrangement, a double slit located in a three-dimensional space. It requires a minimum of two dimensions to detect this effect so that the flux-enclosing region provides a multiply connected domain for the topological enclosure of the flux to be realized. The vector potential-induced phase shift responsible for the A–B effect then involves the total flux enclosed in the region. The flux-containing region must exist in the path of the two electron waves emanating from the two slits.

   The detection of the macro-scale effect, on the other hand, is effected in one dimension along the magnetic field, and is mediated through the macro-scale matter waves, which are identified with the quantum modulation of the de Boglie wave itself. It is not necessary for the flux-containing region to be in the path of the electron beam. It is only required that a (curl-free) vector potential field exists in the region of passage of the electron beam. Thus, the toroid enclosing the flux exists completely outside the experimental chamber in the experiment reported. There is no topological flux enclosure here, and as explained earlier (and elaborated in [6]), the phase shift responsible for the detection on the macro-scale involves only a fraction G of the total flux Φ, determined by the line integral of the vector potential field over a finite 'open' path length—the fraction G being determined by the length of the path.
3. The vector potential-induced phase shift in the A–B case is entirely independent of the electron energy, while the macro-scale one depends not only on the energy (as demonstrated in figure 2(A)), but also on a geometrical factor G, which depends on the position of the grid in a particular run of the experiment. This is demonstrated through figure 4(B).

4.1. On the question of gauge invariance

The macro-scale detection of the vector potential, which has been shown to be effected in one dimension, has involved open paths and the path difference of these open paths along the magnetic field along which the line integrals of the vector potential have been evaluated, and corresponding phase shifts determined. The occurrence of the 'open paths' in the

above formalism may cause some disquiet in some quarters because of the question of the 'gauge invariance' of the results obtained. The situation here gets compared with the A–B case where the phase shift is seen to be trivially gauge invariant, because of the topological enclosure of the flux by the two interfering paths.

True, to ensure that there is no ambiguity and arbitrariness in the determination of the phase shifts, or any other result for that matter, arising out of the arbitrariness of the vector potential, it is generally demanded that the result, and in the present case, the phase shift so determined is 'gauge invariant'. However, at times there seems to reign some confusion with respect to such a requirement. It needs to be emphasized that once a gauge has been chosen in a particular calculation, appropriate for the particular situation, there is no more gauge freedom left, and no further demand is warranted for the result to be 'gauge invariant'. However, sometimes such questions are posed which betray a sense of confusion. For example, if the vector potential field due to a flux density distribution has been determined in the Coulomb gauge (which is appropriate for the static case) satisfying the boundary conditions of its vanishing at infinity, the vector potential field is uniquely determined.

In the present case of macro-scale curl-free vector potential detection, the vector potential field due to the toroidal solenoid employed in the experiment has been evaluated in the Coulomb gauge subject to the boundary condition of its vanishing at infinity, and is thereby uniquely determined. A line integral of this vector potential field along any open path thus has an unambiguous value. There should not therefore exist any doubt about its uniqueness, simply because the line integral is along an open path.

It is true, as noted already, that in the case of the A–B effect, the gauge invariance is trivially satisfied because the interfering paths enclose the entire flux topologically, and the phase shift involves the entire flux in the toroidal solenoid. By contrast, the macro-scale detection alluded to here involves only a fraction G of the total flux Φ contributing to the phase shift, because of the finite length of the open path. An experimental substantiation of the dependence on the geometrical factor G, as mentioned above, testifies to the validity of the above argument.

5. Epilogue

It is to be noted from the above discussion involving the two effects that the A–B effect is actually much simpler to comprehend, in comparison to the macro-scale one, which is seen to be much more subtle. The differences recounted above between the characteristics of the two effects make them quite part from each other. In fact, there is a fundamental difference between the two. It is important to emphasize that they pertain to two entirely different entities.

The A–B effect pertains to the electron as a de Broglie wave, while the corresponding macro-scale effect pertains to the quantum modulation as a macro-scale matter wave. The behaviour of a system resulting from the modulation—the macro-scale matter wave—should be scrupulously distinguished from that attributed to the de Broglie wave, and the former should not be attempted to be understood in terms of the framework of the latter. It cannot be so understood.

However, it may well be debated whether or not it ought be regarded as a quantum effect. If one were to characterize a quantum effect only through the presence of $\hbar$ as a defining characteristic of quantum phenomena, then this effect may not qualify as being quantum. In fact, $\hbar$ is conspicuously absent from the governing Schrödinger-form equation (1), and therefore, also from the effects emanating therefrom. However, the wave nature of the above equation and the various phenomena associated with this, as revealed experimentally, must, nevertheless, be regarded unmistakably as a signature of quantum dynamics, if one recalls that the whole formalism predicting these effects has as its origin, the quantized structure of the energy levels—the Landau levels.

It may thus be concluded that the various observed matter wave effects on the macro-scale, including the vector potential observation, are of quantum origin, but of an entirely different nature, not involving $\hbar$ explicitly. Of course, the manner in which these effects arose would not appear to be manifestly related to quantum dynamics. In fact, far from it! It is for this reason that initially these effects tended not to be believed to be physically valid, since they were seen to be contrary to the current perception on various counts as discussed above.

Another important point that needs to be highlighted about the quantum modulation is that it embeds in it information about the transition that led to its generation. The wavelength of the macro-scale matter wave $\lambda_{\mathrm{M}} = 2\pi v/\Omega$ associated with the modulation is a signature of one Landau level transition that generated it. The observed harmonic peaks in the interference pattern relating to the wavelength $\lambda_{\mathrm{M}}^{(2)} = 2\pi v/2\Omega = \pi v/\Omega$ correspond to two Landau level transitions, and so on. Thus, the wavelengths as deduced from the interference effects contain in them information about the Landau level structure.

In the context of charged particles in an electromagnetic field, it may be concluded in a summarizing comment that the state of an electron in terms of its behaviour is characterized by the environment that it finds itself in. In a macro-scale situation it ordinarily behaves as a 'classical' electron, governed by the Lorentz equation. Accordingly, it is not supposed to be affected by a curl-free vector potential. In a micro-scale situation, it behaves as a 'quantum' electron, with all the associated well-known matter wave properties à la de Broglie, and a Landau energy level structure. In the context of a curl-free vector potential, a quantum electron is now known to be affected à la A–B.

The above-mentioned observational facts—the detection of vector potential on the macro-scale, and macro-scale matter wave interference effects, alluded to above—point to the existence of yet another state of the electron, which arises out of the Landau level structure—a quantum modulated state—which is determined not just by the present environment, but also by the past history of its interaction with the environment. In the present case under discussion, its scattering against a centre, resulting in the transition across Landau levels, leads to a state of the electron which behaves on the macro-scale entirely distinctly from a 'classical' electron. It is this quantum modulated state which accounts for the observation of a curl-free

vector potential on the macro-scale, as recalled above, and other unusual phenomena—the macro-scale matter wave interference effects [10, 11], which are attributed to the quantum modulation.

To be more specific, the quantum modulated state of the electron is described by the set of the Schrödinger-form equations (1), with the infinite set of components $\Psi(n), n = 1, 2, 3, \ldots, \infty$, which correspond to transitions across one, two, three, etc Landau levels from the initial one N defined by $\mu = N\hbar$.

To go back to the remark made in the introduction—can we now pin down which of the earlier entrenched perceptions need to be relaxed in view of the new results obtained on the observability of a static curl-free vector potential? The answer would be as follows.

1. A phenomena observed on the macro-scale is not automatically guaranteed to be classified as 'classical'—governed by classical equations of motion.
2. By the same token, a phenomenon need not necessarily be on the micro-scale and involve $\hbar$ to qualify as being quantum, the low-temperature phenomena of superconductivity and superfluidity being exceptions. This is a rather radical perceptional change that these new observed phenomena would warrant, since they have been demonstrated to be of quantum origin, even as they are observed on the macro-scale, and do not involve $\hbar$ explicitly.
3. Another related perceptional change arising out of these investigations is that a static curl-free vector potential is not such an unphysical entity, even on the macro-scale, as has been made out by the 'classical view'. In fact, it has been demonstrated to be an observable on the macro-scale, although in a rather special manner, as described here, and in more detail in [6].

A deeper perceptional shift that appears to underly these observed effects and the remarks made above about the perceptions that need to be relaxed is that one may take a more integrated view of classical and quantum mechanics, and not treat them as belonging to two immiscible domains with a null intersection. It is important to remark that in the particular case discussed above, namely the curl-free vector potential observation on the macro-scale, it would be difficult to determine *a priori* whether a particular beam of electrons, propagating along the magnetic field in this essentially macro-scale setting of the experiment, is a beam of 'classical' electrons or of quantum modulated ones, as defined above. It can be so determined only after carrying out an appropriate experiment with it. At the same time, what is interesting to note is that the quantum modulated electrons derive their unexpected properties from quantum mechanics itself, although in a rather unfamiliar and unusual manner.

Recognizing the above-mentioned fact, it is good to realize that we have not yet seen the last of the unexpected consequences of quantum mechanics itself. It is, therefore, helpful to have an open mind on what may at first sight appear to be 'strange'. Unfortunately, dogmas, which many a time have a historical origin, still govern our first reaction to a new result. There have been many dogmas, which have resulted in unfortunate delays in the recognition of new ideas—the observability of the vector potential being one which was held up for a long time by the dogma of the Heaviside–Hertz formulation of electromagnetism in terms of the fields, which alone were accordingly sanctioned to be regarded as 'observables' (see, for instance, Wu and Yang [14] and Feynman [5] on these issues), while potentials merely served as convenient devices.

One may well ask whether the kind of novel phenomena reported are specific only to the system of charged particles in a magnetic field.

It will be shown in investigations to be reported later that such phenomena are not peculiar to this system, but would appear to be rather generic. In more general terms, they would require a bound system in association with at least one free degree of freedom.

References

[1] Aharonov Y and Bohm D 1959 *Phys. Rev.* **115** 485
[2] Tonomura A, Osakabe N, Matsuda T, Kawasaki T and Endo J 1986 *Phys. Rev. Lett.* **56** 792
[3] Chambers R G 1960 *Phys. Rev. Lett.* **5** 5
[4] Rousseaux G, Kofman R and Minazzoli O 2008 *Eur. Phys. J.* D **42** 249
[5] Feynman R P, Leighton R and Sands M 1964 *The Feynman Lectures on Physics* vol 2 (Reading, MA: Addison-Wesley) pp 15-7/15-14
[6] Varma R K, Banerjee S B and Ambastha A 2012 *Eur. Phys. J.* D **66** 38
[7] Varma R K, Punithavelu A M and Banerjee S B 2002 *Phys. Lett.* A **303** 114
[8] Varma R K 2001 *Phys. Rev.* E **64** 036608
[9] Varma R K *Eur. Phys. J.* D **66** 39
[10] Varma R K, Punithavelu A M and Banerjee S B 2002 *Phys. Rev.* E **65** 026503
[11] Varma R K and Banerjee S B 2007 *Phys. Scr.* **75** 19
[12] Varma R K 2007 *Pramana—J. Phys.* **69** 901
[13] Varma R K 2010 *Pramana—J. Phys.* **74** 491
[14] Wu A C T and Yang C N 2006 *Int. J. Mod. Phys.* A **21** 3235